Supplemental Materials and Methods

RIMChip Design Concepts The RIMChip design has 5 microchannels for executing 5 distinct assay conditions. Each microchannel has 4 cell capture chambers in which the assays are executed, and so a single assay condition is repeated 4 times. Several key features are designed into each microchannel to facilitate processes such as imaging, cell loading, and reagent flushing and delivery. First, given the distance and intervening material between the fluidic layer and the beta sensing volume, the spatial resolution of the beta camera is 600 μm, and so the nearest edges of neighboring microchambers are separated by ~800 μm to avoid signal overlap (Supplemental Fig. 1). Second, the microchannels are designed so that cells are captured only within the cell capture chambers. Each chamber contains a 7 × 3 waffle-structured array of 200-μm-deep microwells, separated by 30-μm-thick walls. This structure is designed to minimize the shear stress exerted onto cells that are attached to the bottom of microwells when flushing through new medium or reagents. This waffle design also helps maintain the rigidity of the bottom surface. Third, this bottom surface is only 50 μm thick because of the constraint that the assay sensitivity depends on the proximity of the cells to the camera. This thin-floored PDMS chip provides an ~10-fold increase in collected signal over a common glass microscope coverslip. It also means that if a cell is trapped outside the cell capture chamber, that cell will contribute negligible (<3% of the total counts) signal during an assay, since those cells have up to 1 mm of PDMS separating them and the beta camera. Fourth, the microchannel inlet is designed to avoid clogging of the channels by bubbles, clumps of cells, or other debris. It is also designed for ease of use. The microchannel inlets accommodate a 20- to 200-μL pipette tip so that standard microwell procedures may be used for the introduction of cells and reagents. The bubble depletion chamber (Fig. 1) has a volume of 0.95 μL and successfully removes any bubbles that are introduced in the micropipetting steps. The bubble depletion volume is followed by a filtering area of posts that have a tailored depth of between 25 and 35 μm. This dimension is customized for specific cell types. In this study, we designed a 32-μm gap for liposarcoma cell lines and the U87 isogenic cell lines and a 20-μm gap for all suspended cells (which are smaller). The filter design also significantly enhances the hydrodynamic resistance of a channel and prevents backflow at the completion of solution injection. This significantly increases cell loading uniformity. The volumes at the microchannel exits have a size sufficient to hold all the overflow from a given micropipetting step. That overflow is removed also using a micropipette. The region of the RIMChip containing the cell capture chambers has a 1 × 1 cm footprint for matching to the beta-particle camera.

RIMChip Fabrication The microchip is fabricated from 2 layers of the air-permeable elastomer polydimethylsiloxane (PDMS) using standard soft lithography methods. Referring to Supplemental Figure 1, the bottom PDMS layer contains the waffle-structured floor and sidewalls of the cell capture chambers. This layer is molded from a silicon wafer–based master. The features on this master were patterned using photolithography of the negative photoresist SU8 2025 (Microchem). The height of these features is about 50 μm. The top PDMS layer

contains all other features (Supplemental Fig. 1). The mold used to form this top PDMS layer was fabricated differently. We first patterned the filter layer using SU8 2025 with a height of 25 μm and then patterned the second layer of microchannels and cell capture chambers using SU8 2100 (Microchem) on the same wafer. The second patterned layer has a height of 200 μm. This is to ensure that the volume of the cell capture chambers has sufficient nutrients to support captured cells for the duration of the on-chip culturing steps that are required as a part of the Betabox assays.

A precured PDMS mixture with a ratio of 5:1 (precursor to cross-linker) is used to fabricate the top PDMS replica, and 20:1 is used for bottom PDMS replica. After curing both PDMS replicas, we trimmed and punched the top PDMS layer with appropriate inlet and outlet holes at 1.5-mm and 5-mm diameters, respectively, and then aligned and mated the top and bottom PDMS layers. Subsequently, the whole assembly was baked at 80°C overnight to seal those layers together. Finally, the entire microchannel was filled with PBS solution through dead-end filling by exerting 3 psi N_2 pressure in a tubing connected to the microchip.

The beta-particle camera (Betabox). The imaging system is a direct detection beta particle detection camera utilizing a 13.5×13.5 mm^2 active area position-sensitive avalanche photodiode (PSAPD) (Radiation Monitoring Devices). The 5 outputs of the PSAPD first pass through CR-110 charge-sensitive preamplifiers and then shaping amplifiers with a 200-ns shaping time. The shaped sum signal then passes to a threshold comparator that produces event trigger pulses to 4 sample and hold (S/H) circuits (53-ns acquisition time, 6-μs hold time). These circuits then initiate an analog-to-digital conversion of the positioning channels using a simultaneous sampling data acquisition system (DAQ) (National Instruments PCI-6143). Beta distribution images were created using the algorithm proposed by Zhang (*1*).

Surface coating. For adherent cell lines, the microchamber surface was coated with various substrates to test cell adhesion. Fibronectin (BD Biosciences) was used to coat the PDMS microchannel and cell capture chamber surfaces at a variety of concentrations of 1, 0.5, 0.33, and 0.25 mg/mL. Those surfactant solutions were injected into microchannels by pressing a pipette for 30 s and then incubating the RIMChip at least overnight before use. Liposarcoma cells were then loaded into each of the microchannels, and the microchip was incubated in a cell incubator at 37°C for 4 h. Microscopic examination of the trapped cells did not reveal any differences in terms of cell attachment and cell number distributions for these various treatment chemistries. We then executed ^{18}F-FDG Betabox radioassays to investigate whether the various surface-coating conditions influenced glucose metabolism of the captured cells. The result, shown in Supplemental Figure 3A, indicated that the fibronectin coating chemistry also did not significantly influence the radioassay.

We also investigated the influence of incubation time on radioassays for the fibronectin coating. Four microchannels were incubated with 0.25 mg/mL fibronectin in PBS for 1, 2, 3, and 4 d under ambient conditions. Cells were loaded into the 4 microchannels and processed as described

above. Again, we did not observe differences in terms of cell attachment and cell number distribution (Supplemental Fig. 3B), except in the microchannel without the fibronectin treatment. The cells within the uncoated chambers did not appear adherent and spread out, relative to those cells in the fibronectin-coated chambers. However, the attachment apparently did not significantly influence the radioassay result.

Cell-loading statistics. Various cell lines were tested in the RIMChip. Adherent cell lines included liposarcoma LS030609 and its MCT-1 deficient line, liposarcoma 060208 and its dCK knockdown line, and the glioblastoma U87 EGFRvIII PTEN cells. Nonadherent cell lines were murine leukemic lines L1210 and its dCK knockdown line, and the Jurkat T cell line. LS060208 liposarcoma cells showed uniform cell number loading along a channel and across the 4 chambers within a channel (Supplemental Fig. 2). A 9.8%–16.9% variation between the 4 cell capture chambers within 1 microchannel, and 6.5% cell number difference across all microchannels on a RIMChip, was observed when 50–60 cells were loaded per chamber.

Suspension cells attached to the hydrophobic PDMS surface without any coating. Up to 4 h of incubation of L1210 leukemia cells, CEM cells, and Jurkat T cells (all suspension cells) did not result in loss of cell number (Supplemental Figs. 4A and 4B) or viability, indicating that the surface attachment is robust and not cell type–specific. However, the uniformity of the deposited cell distribution is susceptible to the hydrodynamic resistance encountered by the cell suspension as it flows through the channel. This may be minimized by optimizing the inlet filter gap (Fig. 1A). A filter gap of 20 μm was used for studying all the (relatively small) suspension cells, and this improved loading uniformity.

RIMChip radioassay execution. Each RIMChip assay relies on the use of a pipette for all fluidic control. To replace a solution in microchannels, a new solution is introduced through the microchannel inlets. Excess solution is removed at the outlets using a 100-μL pipette. For adherent cells, the RIMChip was prepared with a fibronectin surface coating. Immediately before cell loading, the outlets were drained of solution. Cells at a concentration of 3×10^6/mL were injected into the microchip from inlets by pressing a pipette for 5 s, which is sufficient to cover all microchannels with cells. The outlets were then refilled with cell culture medium to prevent the connected microchannels from drying out during the incubation period. The RIMChip was then placed into a CO_2 incubator at 37°C with 100% humidity for 4 h. After incubation, the microchannels were flushed 2 times with flowing ~20 μL PBS, by pressing a pipette for 30 s, to flush out any residual glucose. About 10 μL 1 mCi/mL ^{18}F-FDG or 0.01 mCi/mL ^{18}F-FAC in PBS was loaded into the microchannels by pressing the pipette for 15 s. The whole microchip was then incubated for 30 min in a CO_2 incubator at 37°C. It was the flushed 2 times with flowing ~20 μL PBS. The RIMChip was then ready for mounting onto the beta camera.

For drug inhibition studies, we introduced the cells onto the RIMChip 4 h before the radioassay. 5 mM 2-deoxyglucose (2DG), 10 μM gemcitabine, or 5 μM erlotinib in RPMI 1640 or DMEM medium supplemented with 10% FBS was then added to the microchannels by pipetting, and

incubated with cells for designated periods. Drug molecules were removed from the microchannels by PBS flushing twice. Immediately following, 1 mCi activity of ^{18}F-FDG in PBS was introduced into the microchambers. Adjacent microchannels were devoted to assay/control pairs, with the control microchannel treated equally to the assay microchannel, except that no drug was added. The signal averaged from the 4 cell capture microchambers within the control microchannel was converted into activity per cell and then used for normalization of the similarly converted signal from the drug-treated cells.

The imaging acquisition time depends on the activity of radioactive probe used for the radioassay, with other experimental conditions set. We used 1 mCi/mL activity of ^{18}F-FDG for tests on both adherent and suspended cells, with a fixed incubation time of 30 min. The imaging acquisition time was set to 5 min. We also explored lowering the dosage of ^{18}F-FAC to 10 μCi/mL for suspended cells and used an acquisition time of 10 min. Even with such low activity, the RIMChip platform still differentiated the leukemic line L1210 from its dCK knockdown line.

Off-chip radioassay. In parallel with on-chip radioassay, off-chip radioassays were performed for each cell sample. Liposarcoma cells were detached from a Petri dish and transferred to a 12-well plate, with each well containing ~10^4 cells. The poly-D-lysine–coated plates were then placed in a CO_2 incubator at 37°C for 4 h to allow for cell attachment to well plate bottom. Ten microcuries of ^{18}F-FDG or ^{18}F-FAC was added to each well, followed by 30-min incubation. Each well was then flushed 2 times with PBS. The cells were then lysed, and the cell lysates were transferred to plastic vials. The radioactivity of each cell sample was measured using a well-type γ-counter (1480 Wizard 3; Perkin Elmer).

Data processing. The radio-image was segmented into 20 rectangular regions of interest (ROIs), each of which overlaps a cell chamber and contains the beta particle counts from that cell chamber. The size of ROIs has been optimized by separate experiments to contain >95% of the beta particle counts from a cell chamber and <5% from neighbor chambers. Beta particle counts of each ROI were quantitated by a custom-written Matlab program. The background level was defined from the averaged beta particle counts from 4 ROIs that covered the 4 cell capture chambers in a microchannel that contained zero cells. For facilitation of cell counting using a fluorescence microscope, we stained cells with nuclear dye Hoechst 33342. A script written in ImageJ was used to automate cell counting. The radioactivity of each ROI was normalized by its cell number, and statistics for a given assay condition were calculated from the 4 repeat assays within a given microchannel. We limited comparisons of absolute beta particle counting results across different experimental conditions to only those assays that were executed simultaneously and on the same RIMChip. To compare the results across different RIMChips, we selected 1 of the 5 microchannels from each RIMChip as a reference, and repeated the same experiment across all RIMChips that were to be compared. The radioactivity of the other microchannels was then normalized to the reference microchannel (Figs. 3A and 3B). This meant that it was not necessary to account for the changing radioactivity from the ^{18}F-labeled radiopharmaceutical imaging probe.

REFERENCE

1. Zhang J, Olcott PD, Levin CS. A new positioning algorithm for position-sensitive avalanche photodiodes. *IEEE Trans Nucl Sci.* 2007;54:433–437.

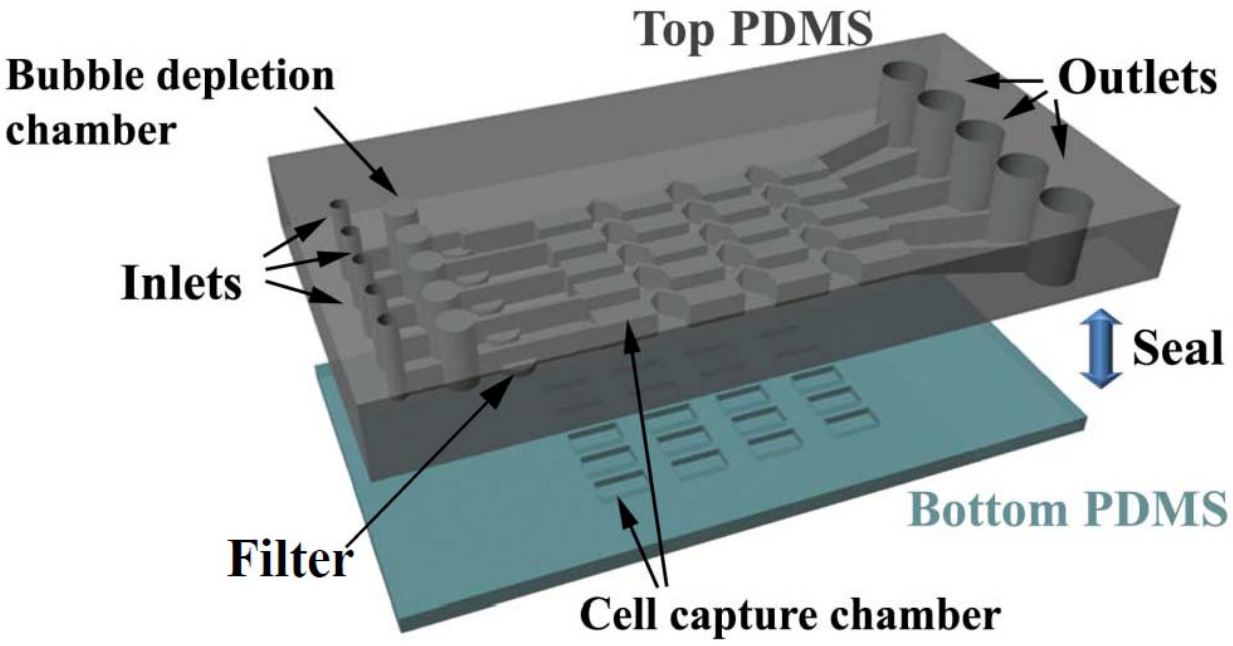

SUPPLEMENTAL FIGURE 1. Fabrication of the RIMChip. The bottom and top polydimethylsilane (PDMS) layers are separately fabricated and then sealed together. Each layer is formed using a mold to shape the curing PDMS. The bottom PDMS layer is molded using a patterned silicon master. The top PDMS layer is molded using a master that is comprised of a patterned multilayer master. Multiple layers of this master are required to generate all of the features of this top PDMS layer. The top PDMS layer contains most of features of a final RIMChip, except walls and waffle-structured floors of the cell capture chambers, which are contained within the bottom PDMS layer.

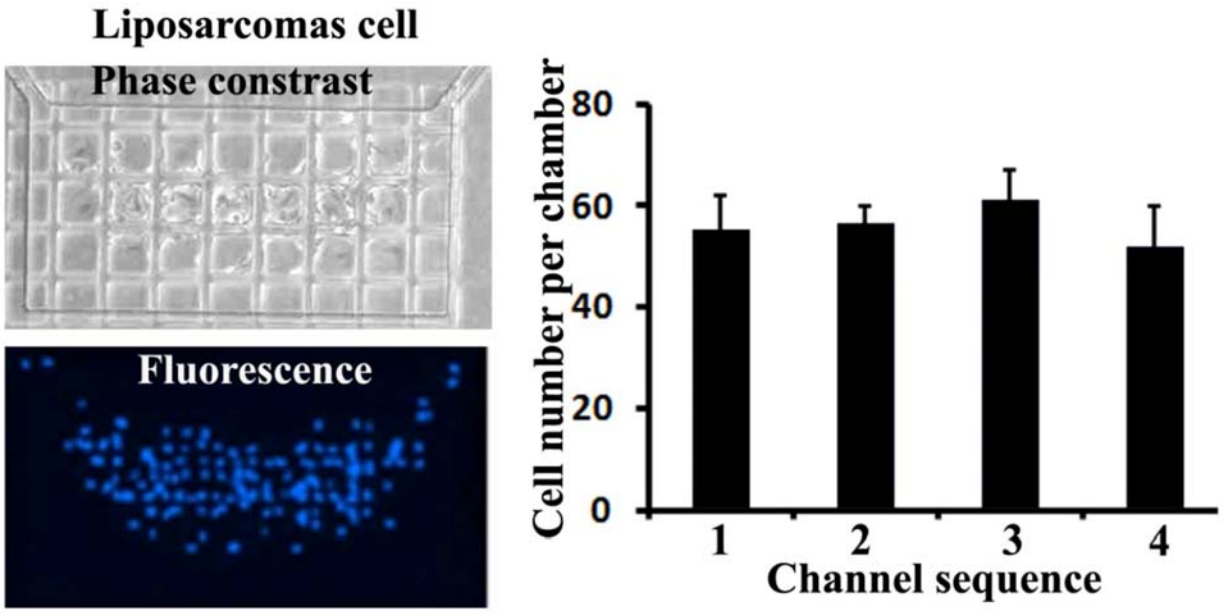

SUPPLEMENTAL FIGURE 2. Distribution of adherent (liposarcoma) cells within fibronectin-coated cell capture microchambers. Each bar in the bar graph represents the averaged cell loading results within the 4 separate microchambers that comprise a single channel. Microscopy images of the capture cells (not shown) reveal that the liposarcoma cells were surface-adherent after 4 h of incubation. Nuclear (fluorescent) staining facilitates cell number counting by fluorescence microscopy and automated counting algorithms.

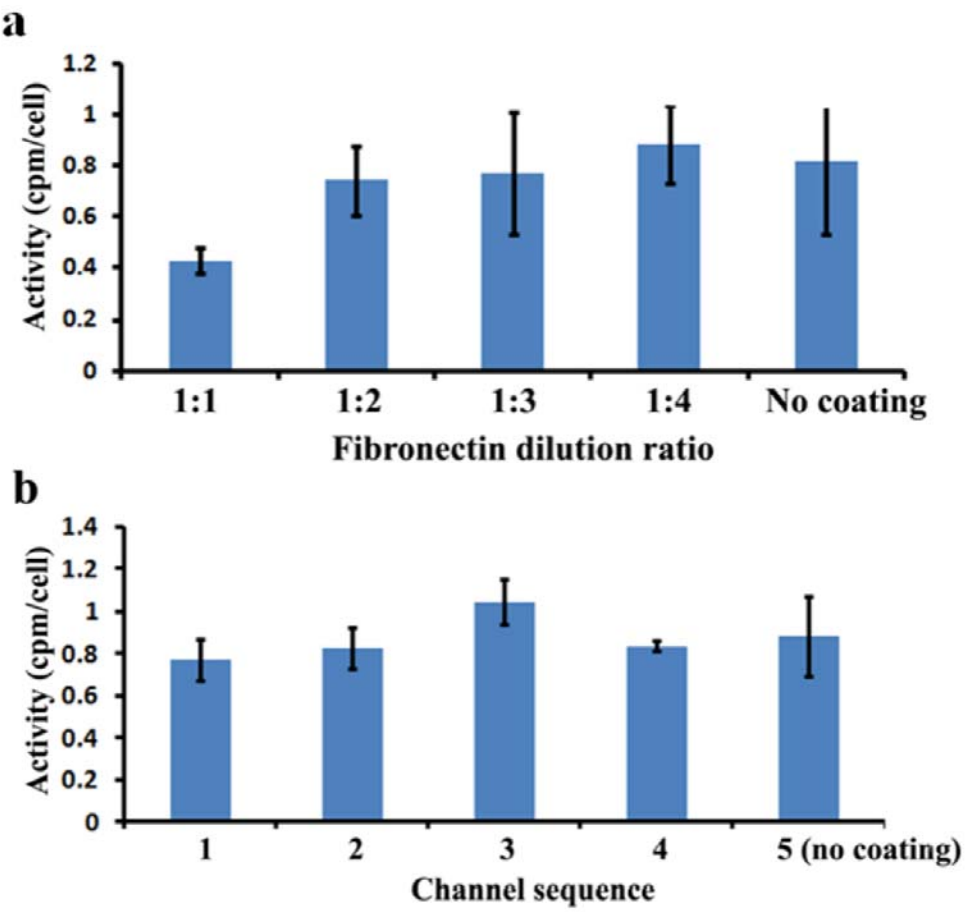

SUPPLEMENTAL FIGURE 3. Effect of fibronectin coating on ^{18}F-FDG uptake by liposarcoma cells. (a) Effect of fibronectin concentration for coating on uptake of ^{18}F-FDG. The initial concentration is 0.25 mg/mL, which is diluted 2 times, 3 times, and 4 times. Cells do not demonstrate a significant difference with respect to ^{18}F-FDG uptake except in the cell chambers coated with the highest concentration of fibronectin. (b) Channels 1, 2, 3, and 4 were coated with fibronectin for 4, 3, 2, and 1 days, respectively. Channel 5 was not coated. Then, cells were loaded into the cell capture chambers and incubated for 4 h. In channel 5, the cells are not as efficiently captured within the cell capture chambers. ^{18}F-FDG was then added according to the described protocols. No significant differences in ^{18}F-FDG uptake per cell were observed between any of the 5 channels, including the noncoated channel 5, although the cells were adherent only in the chambers associated with microchannels 1-4.

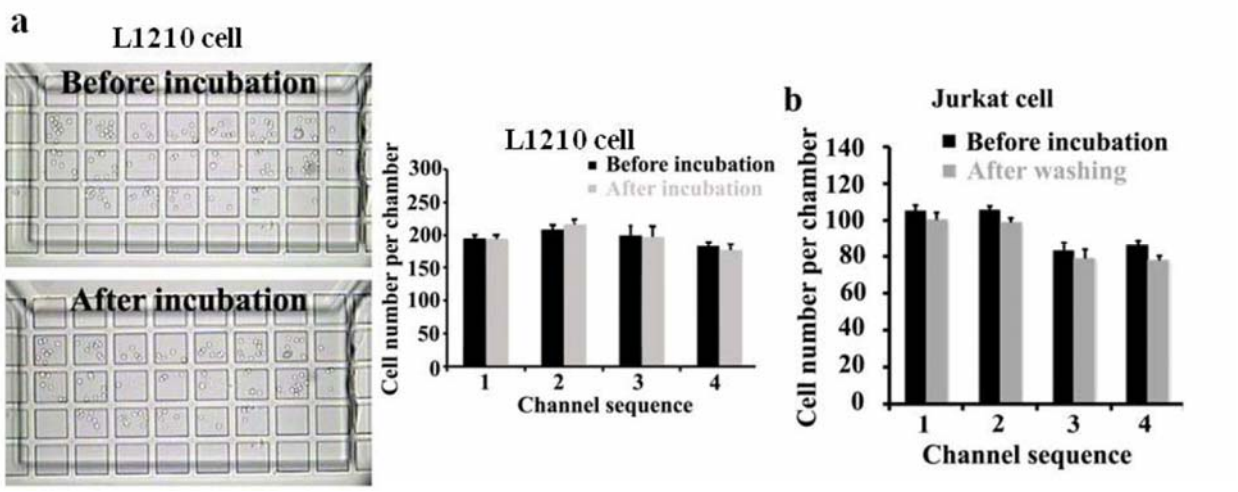

SUPPLEMENTAL FIGURE 4. Uniformity of cell loading within the cell capture chambers of a RIMChip before and after cell incubation and reagent flushing. L1210 lymphoma cells were loaded into 4 of the microchannels of a RIMChip and incubated in RPMI 1640 medium supplemented with 10% FBS for 1 h. The microchannels were then flushed with the various reagents (except a radioimaging probe) to simulate an actual radioassay. Cell number per cell capture microchamber, as well as their positions within the chambers, was recorded before and after the various reagent introductions and flushing steps. As shown for both (a) L1210 cells and (b) Jurkat cells, the various assay steps did not physically influence the cell loading.

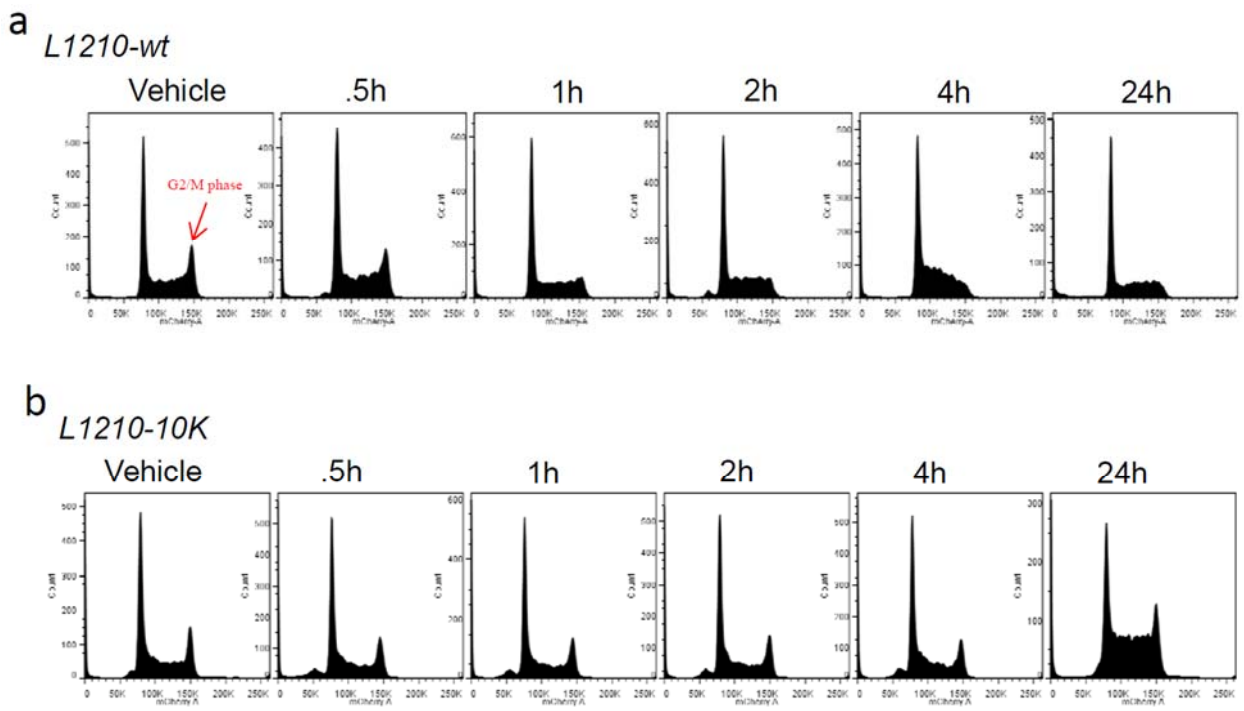

SUPPLEMENTAL FIGURE 5. Proliferation assay on (a) L1210-wt and (b) L1210-10k cells, as measured by flow cytometry. Each cell sample was treated with 10 μM gemcitabine for the indicated durations. The spike at the right of the histograms represents cells in the G2/M phase, and the spike at the left represents the G0 phase.

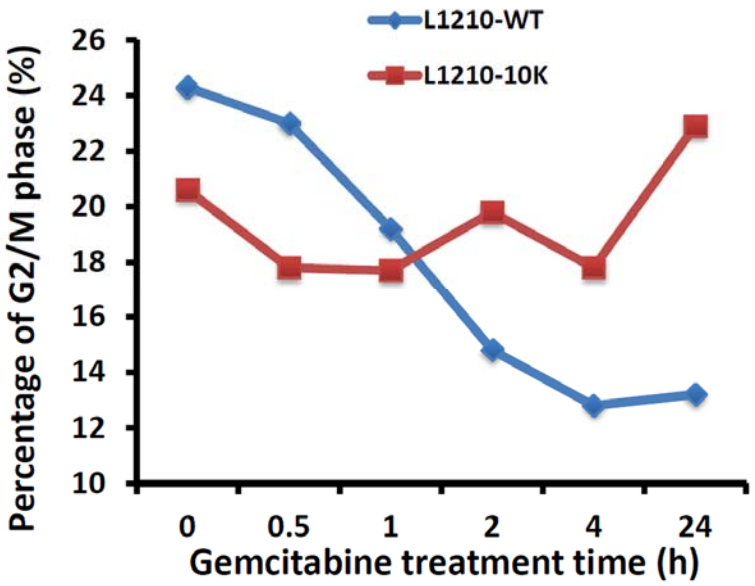

SUPPLEMENTAL FIGURE 6. Quantification of the percentage of cells in the G2/M phase when L1210-wt L1210-10K cells were treated with 10 mM gemcitabine for the designated durations.

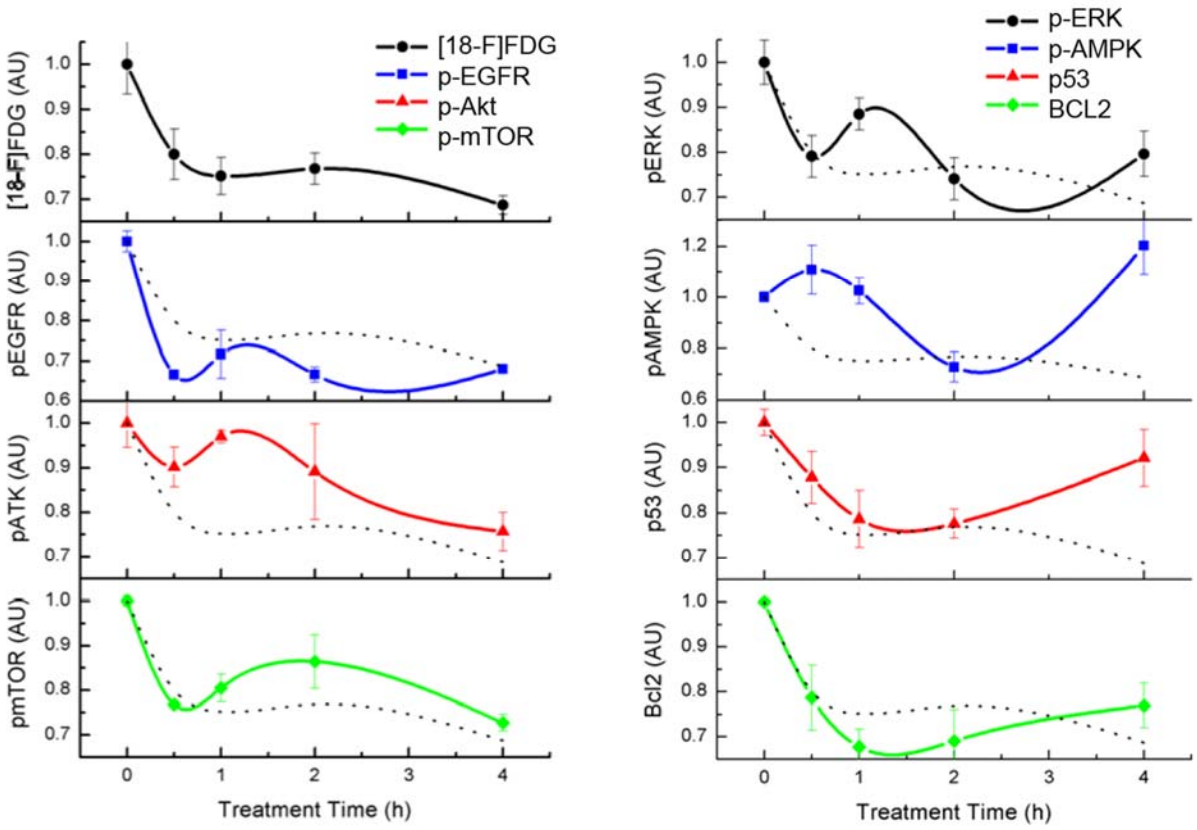

SUPPLEMENTAL FIGURE 7. The kinetics of ^{18}F-FDG uptake, and of the levels of various assayed proteins, as a function of 5 mM erlotinib treatment. The y-axis of these plots reflect the percentage levels relative to 100% at time = 0. Error bars indicate fluctuations of 3 repeats.

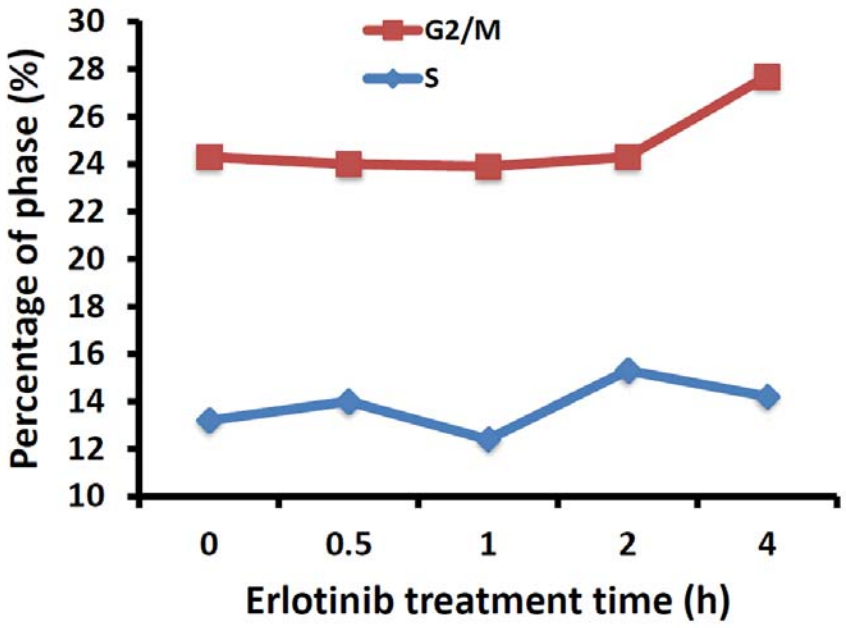

SUPPLEMENTAL FIGURE 8. Kinetics plot, showing the percentage of cells in S and G2/M phases of the cell cycle for U87 EGFR vIII/PTEN cells that were treated with 5 mM erlotinib for the designated durations.

SUPPLEMENTAL TABLE 1. List of Antibodies Used for Protein Assays from the U87 EGFRvIII PTEN Cells

DNA label	Antibody (ventor: clone)	Source
D	mouse anti-hu phospho-EGFR	R&D Y1068
	biotin-labeled goat anti-hu EGFR	R&D BAF231
E	anti-hu phospho-Ampka kit	R&D DYC 3528
F	anti-hu p53 kit	R&D DYC 1746
G	anti-hu Bcl2 kit	R&D DYC 827B
I	anti-hu phospho-mTOR kit	R&D DYC 1665
K	anti-hu phoshpo-ERK kit	R&D DYC 1018B
L	anti-hu phospho-Akt1 kit	R&D DYC 2289